█ Halogen Bonding

Halogen- and Hydrogen-Bonded Salts and Co-crystals Formed from 4-Halo-2,3,5,6-tetrafluorophenol and Cyclic Secondary and Tertiary Amines: Orthogonal and Non-orthogonal Halogen and Hydrogen Bonding, and Synthetic Analogues of Halogen-Bonded Biological Systems

Akihiro Takemura, Linda J. McAllister, Sam Hart, Natalie E. Pridmore, Peter B. Karadakov, Adrian C. Whitwood, and Duncan W. Bruce*[a]

Abstract: Co-crystallisation of, in particular, 4-iodotetrafluorophenol with a series of secondary and tertiary cyclic amines results in deprotonation of the phenol and formation of the corresponding ammonium phenate. Careful examination of the X-ray single-crystal structures shows that the phenate anion develops a C=O double bond and that the C−C bond lengths in the ring suggest a Meissenheimer-like delocalisation. This delocalisation is supported by the geometry of the phenate anion optimised at the MP2(Full) level of theory within the aug-cc-pVDZ basis (aug-cc-pVDZ-PP on I) and by natural bond orbital (NBO) analyses. With sp^2 hybridisation at the phenate oxygen atom, there is strong preference for the formation of two non-covalent interactions with the oxygen sp^2 lone pairs and, in the case of secondary amines, this occurs through hydrogen bonding to the ammonium hydrogen atoms. However, where tertiary amines are concerned, there are insufficient hydrogen atoms available and so an electrophilic iodine atom from a neighbouring 4-iodo- tetrafluorophenate group forms an I···O halogen bond to give the second interaction. However, in some co-crystals with secondary amines, it is also found that in addition to the two hydrogen bonds forming with the phenate oxygen sp^2 lone pairs, there is an additional intermolecular I···O halogen bond in which the electrophilic iodine atom interacts with the C=O π-system. All attempts to reproduce this behaviour with 4-bromotetrafluorophenol were unsuccessful. These structural motifs are significant as they reproduce extremely well, in low-molar-mass synthetic systems, motifs found by Ho and co-workers when examining halogen-bonding interactions in biological systems. The analogy is cemented through the structures of co-crystals of 1,4-diiodotetrafluorobenzene with acetamide and with N-methylbenzamide, which, as designed models, demonstrate the orthogonality of hydrogen and halogen bonding proposed in Ho's biological study.

Introduction

As well as being a now widely used tool in supramolecular chemistry,[1–5] halogen bonding has been used in the formation of liquid crystals,[6] and is implied in studies in, for example, non-linear optics,[7,8] gels,[9] anion recognition,[10] magnetic and conducting materials,[11] separation of α,ω-diiodoalkanes,[12] porous materials[13,14] and catalysis.[15] As is well known, halogen-bonding interactions tend to be strongest with the most polarisable halogens, namely bromine and iodine, and to some extent this has slowed its extension into the arena of biology.[16] Thus, whereas iodine is an essential trace element owing to its role in thyroid hormones in animals, bromine is not an essential element and its functions can be replaced by chlorine when it is not available.

Nonetheless, there are many known halogenated metabolites including antibiotics and it is also known that certain inflammatory responses can lead to oxidative halogenation of proteins and amino acids. The possible structural role of halogens in biological systems has been looked at in some detail by Ho and co-workers,[17] who identified a dominant interaction, namely the approach of the halogen atom to the π-system of the carboxyl oxygen atom of an amide link—an interaction that had little precedent in the literature. These authors then went on to show how hydrogen and halogen bonds to such carbonyl oxygen atoms could be regarded as orthogonal, providing examples where both were found simultaneously.[18] These important, original studies have led to wider interest.[19]

[a] A. Takemura, L. J. McAllister, S. Hart, N. E. Pridmore, Dr. P. B. Karadakov,
Dr. A. C. Whitwood, Prof. Dr. D. W. Bruce
Department of Chemistry, University of York
Heslington, York YO10 5DD (UK)
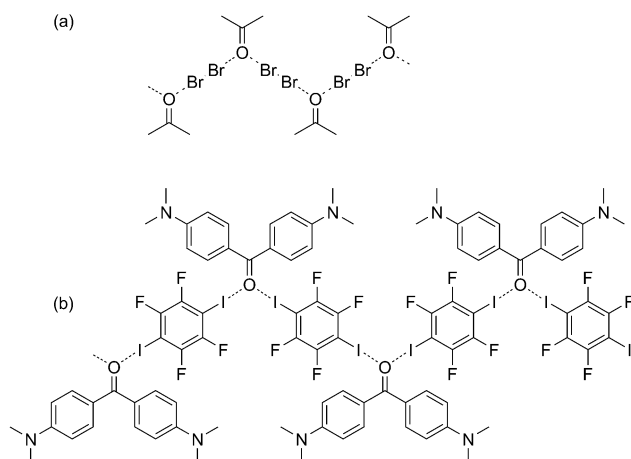E-mail: duncan.bruce@york.ac.uk

Figure 1. Halogen-bonding interactions with ketones. The interaction motif found in (a) acetone/Br$_2$ and (b) 1,4-diiodotetrafluorobenzene with a bis-4-(N,N-dimethylamino)benzophenone.

The study of interactions of halogens with carbonyl oxygen atoms goes back to the work of Hassel and Strømme who, in 1959, described the formation of a polymer between Br$_2$ and acetone,[20] where bromine bridged between two acetone molecules to form the repeating motif (Figure 1). The angle at the oxygen atom was reported as 110°, whereas the Br-Br-O angles were strictly linear. The motif would suggest that the oxygen atom uses sp^2 orbitals in the bonding, although a recent theoretical study questions this.[21] A similar polymeric motif is described when the ketone is found in 4,4′-bis(N,N-dimethylamino)benzophenone and the dihalogen is 1,4-diiodotetrafluorobenzene.[22]

More recently, intermolecular C=O···Br interactions were found to direct the crystal structures of o-bromoaromatic aldehydes,[23] whereas halogen bonding between carbonyl oxygen atoms and bromine has been found to induce phosphorescence in organic compounds, namely with 2,5-dihexyloxy-4-bromobenzaldhyde[24] and a tert-butoxycarbonyl (Boc)- and N,N-dicyclohexylurea-capped γ-amino acid with a bromo substituent.[25]

Described as a 'small-molecule analogue' of the orthogonal interactions observed in biological systems, El-Sheshtawy et al. reported the structures of a cucurbit[6]uril containing either Br$_2$ or I$_2$ inside the cavity.[26] However, examination of the lengths of the I···O and Br···O separations (99% of the sum of the van der Waals radii), the magnitudes of the I—I···O and Br—Br···O angles (major deviations from linearity) and the space-filling model rather suggest a simple inclusion complex stabilised by weak dispersion forces.

The molecule 4-iodotetrafluorophenol can act as both halogen-bond and hydrogen-bond donor. The phenol readily forms 2:1 complexes with 4-alkoxystilbazoles that have liquid crystal properties,[27] but use of a 1:1 ratio of the two components leads to a 1:1 co-crystal in which the stilbazole hydrogen bonds preferentially to the iodophenol. However, the extremely electrophilic nature of iodine clearly demands electron density and the single-crystal structure showed a halogen bond between the iodine atom and the ether oxygen atom of a neighbouring stilbazole, forming a non-covalent, polymeric motif. Interested then to explore further the balance between hydrogen and halogen bonding in this phenol, we produced a number of co-crystals with cyclic secondary and tertiary amines and in so doing, provided low-molar-mass analogues of the halogen-bond motifs found in biology as described by Ho and co-workers.[17,18]

Results

Crystal and molecular structures

Crystals were produced by co-crystallising 4-iodotetrafluorophenol, 4-bromotetrafluorophenol or pentafluorophenol with the appropriate base in the solvent/anti-solvent system given in Table 2, typically using base/phenol ratios of 1:1. The new salts and co-crystals are shown in Figure 2 and crystallographic data are collected in Table S1 in the Supporting Information.

Salts of pentafluorophenol

Piperidinium pentafluorophenate (1)

The complex crystallised with the expected 1:1 stoichiometry and the positions of the hydrogen atoms on the nitrogen were confirmed by difference mapping, whereas all the positions of all other hydrogen atoms were calculated and refined by using a riding model. The piperidine deprotonated the pentafluorophenol (in contrast to the co-crystal with aniline where both components were neutral[28]) and the crystallised salt exists as a 2:2 dimer in which two of the phenate anions are held together by hydrogen bonds to the two N—H hydrogen atoms on each of the secondary ammonium cations (Figure 3a). This gives a bifurcated motif at oxygen and leads to the formation of a hydrogen-bonded, eight-membered ring arrangement involving two nitrogen atoms, two oxygen atoms and four hydrogen atoms, in which all atoms are close to being co-planar. The two oxygen atoms are not opposed directly and the C-O···O angle is found to be 173.95°. The N—H lengths are equivalent at about 1.8 Å and the two hydrogen atoms binding to oxygen make an angle of 96.32°.

The structure propagates in the direction perpendicular to the fluorophenyl rings, which stack upon one another with a plane-to-plane separation of 3.310 Å to give the motif shown in Figure 3b. The apparent 'voids' to either side of the main stack are occupied by neighbouring stacks that are out of register.

4-(N,N-Dimethylamino)pyridinium pentafluorophenate···pentafluorophenol (2) and 4-(pyrrolidino)pyridinium pentafluorophenate···pentafluorophenol (3)

As expected, in 2 the phenol is deprotonated by the 4-(N,N′-dimethylamino)pyridine (DMAP) and the N—H hydrogen atom forms a hydrogen bond to the phenate oxygen atom at a distance of 1.84(2) Å. However, examination of the structure reveals that it crystallises with an additional molecule of penta-

fluorophenol and that this phenolic hydrogen atom forms a hydrogen bond to the oxygen atom of the phenate anion, a hydrogen bond that, at 1.68(3) Å, is just shorter statistically than that to the pyridinium hydrogen atom (Figure 4). The dihedral angle between the aromatic ring and the phenolic hydrogen atom is 9(1)°, whereas it is 25.4(8)° when the N–H hydrogen atom is considered; the angle made at the phenate oxygen atom by the two hydrogen-bonded hydrogen atoms is 119(1)°. Also of note is that the angle made between the planes of the two phenolic rings makes them close to co-planar (8.5°), whereas the [DMAPH]$^+$ ring makes an angle of 68.03° to the phenate ring (Figure S1a in the Supporting Information).

In **3**, the phenol is again deprotonated by the tertiary amine and, in common with the structure of **2**, the cation–anion pair co-crystallise with a molecule of pentafluorophenol (Figure 4b). The O–H···O hydrogen bond at a value of 1.56(3) Å is again shorter than the N–H···O hydrogen bond at 1.79(2) Å. In this structure, the cation ring is now closer to the plane of the phenate ring with the two intersecting with an angle of 17.85° and the two phenolic rings making a larger angle of 46.94° (Figure S1b in the Supporting Information).

Salts of 4-iodo-2-3-5-6-tetrafluorophenol

Piperazine-1,4-diium 4-iodotetrafluorophenate (4)

The complex crystallised as a 2:1 (anion/cation) salt as both nitrogen atoms of the piperazine were protonated to give a dication. The basic motif is described by a polymeric arrangement in which two 'opposing' phenates are held together by two piperazine dications with a cationic NH$_2^+$ group hydrogen bonding to the two oxygen atoms ($d_{O···H} = 1.774(1)$ and $1.863(1)$ Å—there is a formal inversion centre), giving an eight-membered ring embracing two dications and two
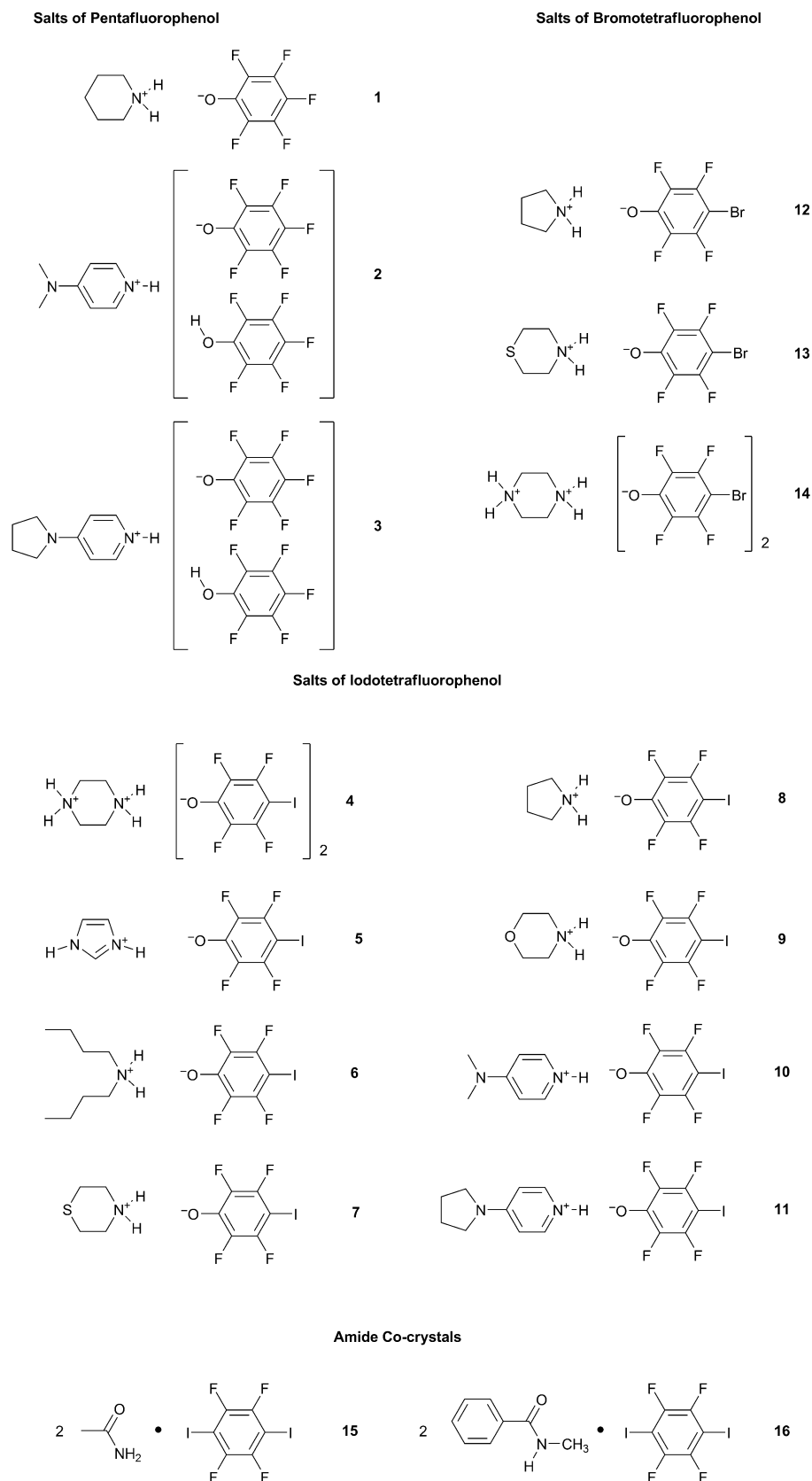

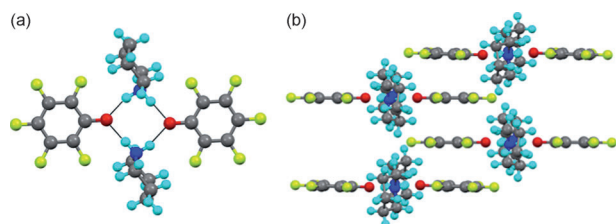**Figure 2.** Molecular formulae of the salts and co-crystals described in this paper.

Figure 3. (a) Hydrogen-bonded [2+2] dimer of salt **1** (hydrogen bonds drawn in black). (b) Packing motif in **1**.
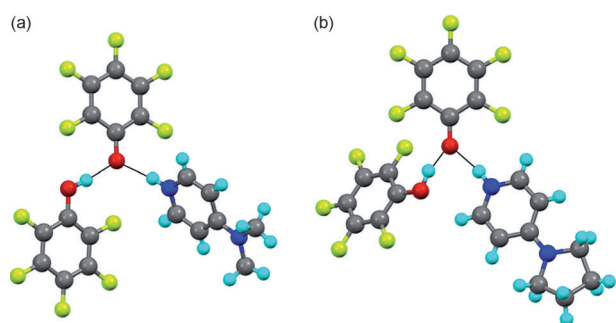

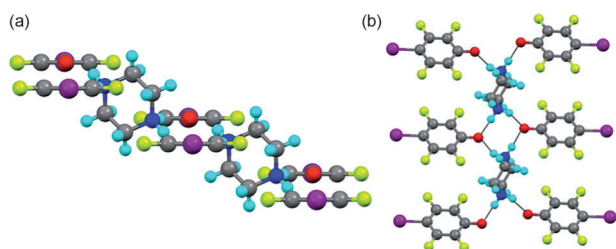**Figure 4.** Molecular structures of (a) **2** and (b) **3**.

Figure 5. Two views of the polymeric motif of complex **4**: (a) Side view and (b) top view.

phenates with the H···O···H angle as 107.37(7)°. Note that the two aromatic rings are not coplanar (Figure 5 a). The other end of each dication participates in an identical bonding pattern, leading to the basic polymeric unit (Figure 5 b) and it can be seen that the aromatic rings form a staircase-like arrangement. Other details of the crystal packing in **4** are shown in Figure S2 (see the Supporting Information).

Imidazolium iodotetrafluorophenate (5)

The asymmetric unit contained two pairs of molecules, which were related symmetrically by a 180° rotation, although the axis of rotation did not correspond to a crystallographic axis. C−H hydrogen atoms were placed by using a riding model, with the acidic hydrogen atoms being located by difference mapping after all other atoms were located and refined.

The structure propagates as a hydrogen-bonded polymer with the hydrogen bonding describing a bifurcated motif at each phenate oxygen atom, of which are of two types. Thus, in Figure 6, all of the hydrogen bonds shown are statistically
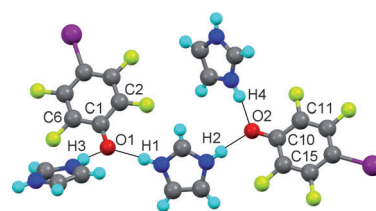

Figure 6. The basic polymeric repeat unit in **5**.

the same length (approximately 1.8 Å), but the torsion angles with respect to the six-membered ring differ. Thus, the torsions described by C11-C10-O2-H4 and by C15-C10-O2-H2 are 10(3)° and 3(3)°, respectively, whereas those described by C1-C2-O1-H1 and by C6-C1-O1-H3 are 16(3)° and 44(3)°, respectively. The less planar arrangement at O1 is understood as there is a long contact (2.434(3) Å) to the C−H (on the C4 carbon) of a neighbouring imidazole (Figure S3 in the Supporting Information), which sits with a torsion angle of 53.3(4)° with respect to C6-C1-O1. There is no such interaction at O2. The two H···O···H angles are also different, with that at O2 being 104(3)° whereas that at O1 is larger at 116(3)°. Further details of the crystal packing are found in the Supporting Information and in Figure S4.

Dibutylammonium iodotetrafluorophenate (6)

Dibutylammonium iodotetrafluorophenate crystallised in the space group I_2/m as a simple 1:1 salt in which two cations and two anions hydrogen bond together to form an eight-membered ring. Two views are shown in Figure 7, with Figure 7 a showing the antiperiplanar arrangement in the dibutylammonium cation, which is, perhaps, better viewed as a 4-azanonane. The packing arrangement is shown in Figure S5 (see the Supporting Information).
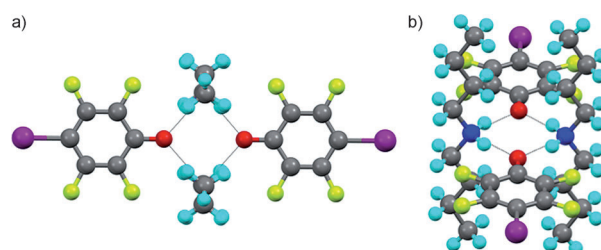

Figure 7. Two views of the hydrogen-bonded unit in **6**: (a) View looking down the 'axis' of the dibutylammonium chains and (b) at an angle to show the N−H···O hydrogen bonds.

Thiomorpholinium iodotetrafluorophenate (7)

The material crystallised as a 1:1 salt and, in common with the structures of the imidazolium and piperazine-1,4-diium salts of iodotetrafluorophenol, the basic structural motif showed a bifurcated motif for the hydrogen bonding at the oxygen atoms. Also in common with the salt of piperazine, the second hydrogen atom of the secondary ammonium cation took part in
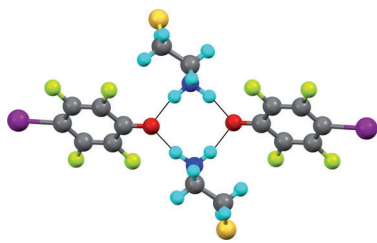
Figure 8. The hydrogen-bonded motif in **7**.

a similar interaction to give a hydrogen-bonded, eight-membered ring (Figure 8). Although not different statistically, the hydrogen-bond lengths are noted as 1.85(2) and 1.71(3) Å and the H···O···H angle is 106(1)°.

Assembly of this dimeric arrangement into a polymeric structure now brings halogen bonding into play, so that the iodine atoms interact with the thiomorpholinium sulfur atoms of neighbouring dimers to give the arrangement shown in Figure 9. The S···I separation is 3.3085(6) Å (87.5% of the sum
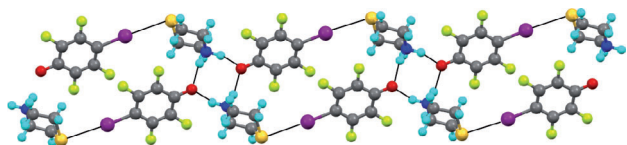

Figure 9. Polymeric arrangement in **7** viewed down the *b* axis and showing the I···S halogen bonds.

of the two van der Waals radii) and the halogen-bond angle at iodine is 172.19(5)°. The directionality of the interaction with sulfur is consistent with a classical view of the position of non-bonded (lone) pairs of electrons on the sulfur atoms, although it should be noted that the C-S···I angles are unsymmetric, being found at 87.81(7)° and 107.79(7)°. The polymer propagates in the *ac* plane and there are no structurally significant interactions to neighbouring chains in either the *a* or *b* directions.

Pyrrolidinium iodotetrafluorophenate (8)

Being the salt of a secondary amine, this material forms the expected dimer supported by hydrogen bonding (Figure 10a)
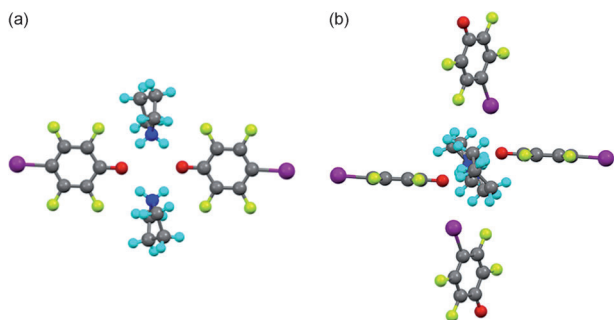

Figure 10. (a) The hydrogen-bonded dimer in **8**. (b) Side view of the dimer showing the I···O halogen bonds.

between the ammonium hydrogen atoms and two phenate oxygen atoms with $d_{H···O} = 1.79$ Å and H···O···H angle of 94°. However, what is totally unexpected is that each oxygen atom also forms a halogen bond with iodine perpendicular to the plane of the phenate anion and, as shown in Figure 10b, one of these halogen bonds is above the plane of the dimer and the other below it. In each case, the halogen bond length is 3.043(1) Å—87% of the sum of the van der Waals radii.

The directionality of the halogen bond is shown in Figure 11, where the two torsion angles made with respect to the plane of the anion ring can be seen. The torsion angle illustrated by Figure 11a and measured with respect to the normal to the ring is found to be 16.5°, whereas the C-O···I angle (Figure 11b) is 105.2(1)°. Details of the crystal packing of **8**, which shows an interesting grid structure defined by the anions, are found in the Supporting Information and in Figures S6–8.
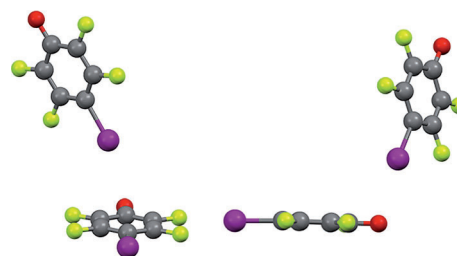

Figure 11. Two views illustrating the directionality of the I···O halogen bond in **8**.

Morpholinium iodotetrafluorophenate (9)

In common with the above structures, a hydrogen-bonded dimer is formed involving two cations and two anions, except that in **9** these dimers are distinct. In each case there are hydrogen-bond lengths of 1.93(3) and 1.77(3) Å; the hydrogen bonds are equal statistically, but differ in the H···O···H angles, which take the values 93° and 103°. In common with the structure of the pyrrolidinium salt **8**, I···O halogen bonds are found (Figure 12) and it was found that halogen bonding involves
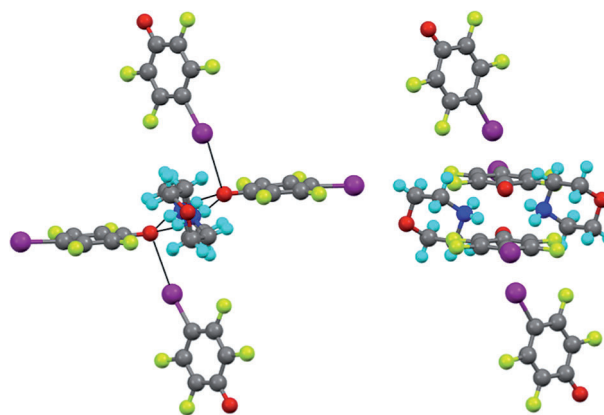

Figure 12. Two views of the halogen-bonding interactions in the hydrogen-bonded cation–anion dimers in **9**. The two views relate to one another through a 90° rotation.

only the cation–anion rings that have the more acute angle. Thus, it is in these dimers that the phenate oxygen atoms interact to form halogen bonds and it is the iodine atoms of the same phenate anion that interact with subsequent dimers forming halogen bonds. There are no close contacts involving the other, distinct cation–anion dimer. The I···O halogen bonds are found to be 3.053(1) Å in length (87% of the sum of the van der Waals radii) and the C-I···O angle is 164.06(5)°. The crystal packing in **9**, which also shows an anion-grid structure akin to that in **8**, is described in the Supporting Information and in Figure S9.

4-(N,N-Dimethylamino)pyridinium iodotetrafluorophenate (10) and 4-(pyrrolidino)pyridinium iodotetrafluorophenate (11)

Being a tertiary amine, protonated DMAP offers only one hydrogen atom for hydrogen bonding, which binds to the phenate oxygen atom in the plane of the iodotetrafluorophenate ring. As found earlier with salts **2** and **3**, the phenate oxygen atom clearly prefers to bind to two electrophilic entities and so in the absence of another hydrogen atom, this role is fulfilled by the iodine atom of a neighbouring phenate anion to give the arrangement shown in Figure 13 a, where $d_{I···O} = 2.993(1)$ Å
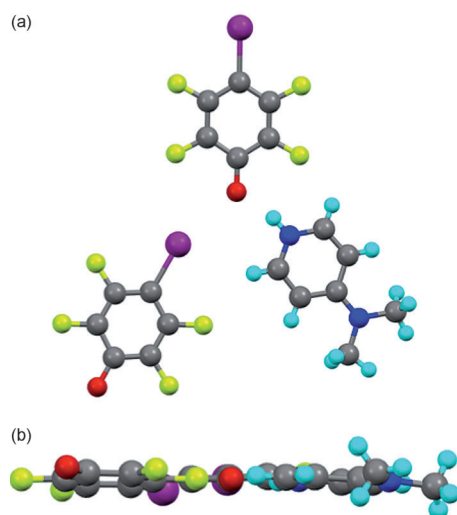

Figure 13. (a) View of complex **10** showing the O···H hydrogen bond and I···O halogen bond. (b) The same unit viewed from the side to show its planarity.

(85% of the sum of the van der Waals radii) and $d_{O···H} = 1.76(2)$ Å; the I···O···H angle is 100.1(8)°. Figure 13 b shows the planarity of the arrangement in **10**. In fact, there are two complexes in the unit cell and whereas the hydrogen-bond lengths are the same in each case, the other halogen bond is slightly shorter at 2.973(1) Å, although the I···O···H angle remains unchanged at 100.1(8)°. The 2D packing is shown in Figure S10 (see the Supporting Information).

A topologically similar motif has been reported recently by Aakeröy et al.[29] in co-crystals of 4-iodotetrafluorophenol with 3,3′-azobipyridine, although in this case the phenol remains
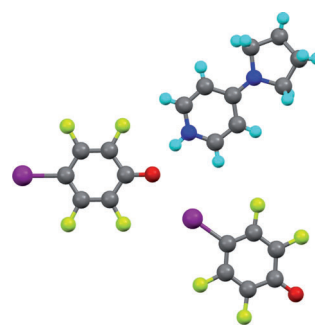

Figure 14. Partial structure of **11** showing both the hydrogen- and halogen-bonding interactions.

protonated and the I···O distance is longer at 3.091(10) Å, no doubt owing to its interaction with the neutral phenol rather than the anionic phenate ligand.

Containing the 4-(pyrrolidino)pyridinium cation, **11** crystallised in a manner similar to that of **10** (Figure 14); the N···H hydrogen bond is 1.79(4) Å long, whereas the O···I halogen bond is found to be 2.884(2) Å. This latter distance is 82% of the sum of the van der Waals radii and so slightly shorter than that in **11**; the I···O···H angle is 100(1)°. The packing is also similar to that in **11** and is shown in Figure S11 (see the Supporting Information).

Salts of 4-bromo-2,3,5,6-tetrafluorophenol

Pyrrolidinium bromotetrafluorophenate (12)

The material crystallised as a 1:1 salt and shows the now-familiar eight-membered, hydrogen-bonded ring with a bifurcated hydrogen bonding motif at the phenate oxygen atoms (Figure 15); the hydrogen-bond length is about 1.87 Å with the H···O···H angle being 105(1)°.
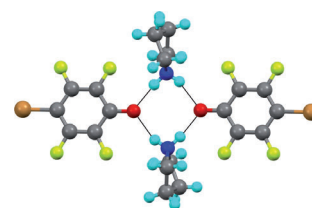
Figure 15. Arrangement of the hydrogen-bonded dimer of **12**.

The propagation of the structure is shown in Figure S12 (see the Supporting Information) and it is noted that there are no significant, intermolecular, structure-directing interactions and no short contacts to bromine.

Thiomorpholinium bromotetrafluorophenate (13)

This material crystallises as the 1:1 salt, but although it shows the same topological pattern of hydrogen bonding at the phenate oxygen atom, this leads to formation of a linear polymer and the eight-membered ring observed in all of the other

Figure 16. The linear, hydrogen-bonded polymeric arrangement in **13**.

structures of salts of secondary amines is absent (Figure 16). More than that, the angle made at the oxygen atom by the two ammonium hydrogen atoms is 136(1)°, whereas in the structure of thiomorpholinium iodotetrafluorophenate (**7**) it is 106(1)° and for pyrrolidinium bromotetrafluorophenate (**12**) it is 105(1)°.

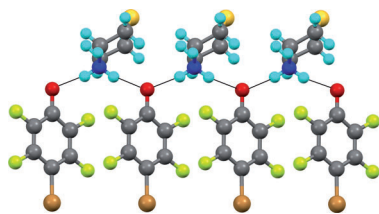The structure propagates as shown in Figure 17a, whereby there are Br···Br interactions with a Type 1 geometry, with the Br···Br distance being found to be 3.3967(4) Å (92% of twice
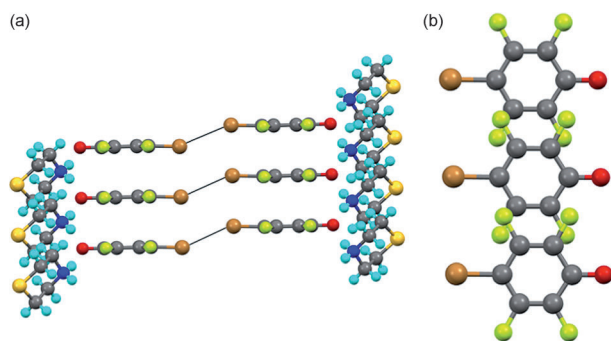

Figure 17. (a) Side-on view of the extended structure of **13** showing the Type I Br···Br interactions. (b) Top view showing only the relative positions of the bromotetrafluorophenate anions.

the van der Waals radius) and with an interaction angle at bromine of 155.83(6)°. However, Figure 17a is slightly misleading as it is not the case that the different bromotetrafluorophenate rings are stacked one upon the other, rather they are slipped with respect to one another, which is illustrated in Figure 17b. The distance between the planes described by the anion rings is 3.039 Å.

Piperazine-1,4-diium 4-bromotetrafluorophenate (14)

This salt is all but isomorphous and isostructural with its iodo analogue (**3**) and is not discussed further save to say that there are no short contacts to bromine. Illustrative diagrams appear in Figure S13 (see the Supporting Information).

Co-crystals of 1,4-diiodotetrafluorobenzene with amides

Acetamide/1,4-diiodotetrafluorobenzene (15)

The crystallisation was set up with *N*-methylacetamide and 1,4-diiodotetrafluorobenzene, but adventitious water caused hydrolysis to acetamide, which crystallised as a 2:1 co-crystal
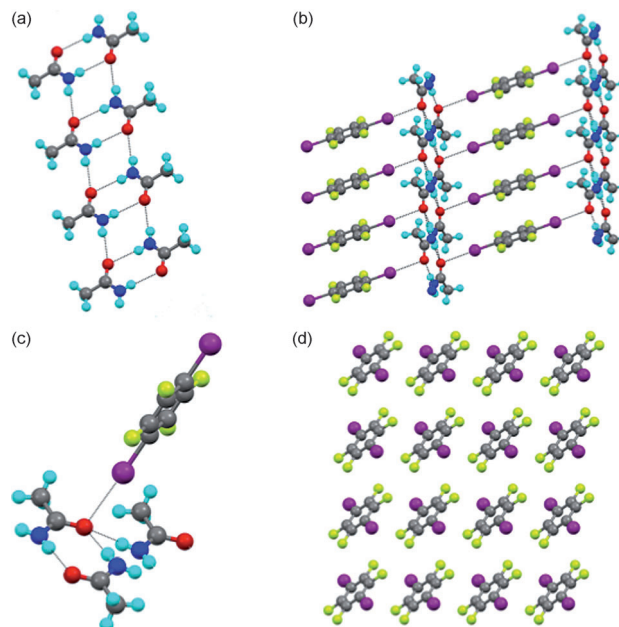

Figure 18. Aspects of the structure of **15**: (a) Hydrogen-bonded sheet formed by acetamide; (b) linking of the hydrogen-bonded acetamide sheets by halogen bonding to 1,4-diiodotetrafluorobenzene; (c) 'close-up' showing the hydrogen and halogen bonding at the amide oxygen atom; (d) packing of 1,4-diiodotetrafluorobenzene viewed down the *c* axis.

(amide/diiodotetrafluorobenzene). As seen in Figure 18a, the amide forms hydrogen-bonded sheets with the N–H hydrogen atoms and the carbonyl oxygen atoms, constituting the now topologically familiar eight-membered ring structure that arises from the arrangement of hydrogen-bonded, dimeric acetamide units. This arrangement is distinct from those found in the two crystal polymorphs of acetamide itself.[30] The N···H separations are 2.06(3) and 2.16(3) Å with the H···O···H angle of 76(1)°. These sheets are then held together through halogen bonding as shown in Figure 18b, with the detail of the interaction of an iodine atom with the amide oxygen atom shown in Figure 18c. The I···O halogen bond length is 2.973(2) Å (84.9% of the sum of the van der Waals radii) with the C-I···O angle being 176.54(8)°. There are two H···O···I angles of 90.9(8)° and 86.5(9)°, whereas the C-O···I angle is 111.3(1)°. The packing of the 1,4-diiodobenzene units is shown in Figure 18d, viewed as looking down the *c* axis. The separation of the planes defined by the aromatic rings is 3.294 Å, although there are no short, inter-planar interactions.

N-Methylbenzamide/1,4-diiodotetrafluorobenzene (16)

The co-crystals formed also have a 2:1 *N*-methylbenzamide/diiodotetrafluorobenzene stoichiometry, but with one proton fewer than **15**; it forms a one-dimensional chain through hydrogen bonding between the amide hydrogen atom and the carbonyl group of an adjacent amide. The aromatic rings do not sit one upon another, rather they propagate through the crystal in a stepped arrangement, with the rings being formally co-parallel every second molecule with a measured separation of 6.348 Å. This differs from the structure of *N*-methylbenza-
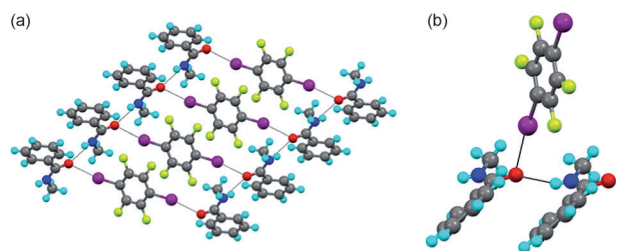
Figure 19. Structure of **19** showing (a) the linear, hydrogen-bonded motif of the methylbenzamide linked by 1,4-diiodotetrafluorobenzene and (b) detail of the hydrogen and halogen bonding at the amide carbonyl oxygen atom.

mide itself, where the aromatic rings alternate from one side of the hydrogen-bonded chain to the other.[31] Pairs of these chains are then bridged by molecules of 1,4-diiodotetrafluorobenzene (Figure 19a), which form an I···O halogen bond in which the I···O separation is 2.884(3) Å (82.4% of the sum of the van der Waals radii) with a C-I···O angle of 169.54(9)° and an I···O···H angle of 83.0(9)°. Note that in this case, the reduced number of hydrogen atoms available for hydrogen bonding means that each oxygen atom interacts with only one hydrogen atom and one iodine atom (Figure 19b), whereas in **15** there are two interactions with two hydrogen atoms. The crystal packing in **16** is illustrated in Figure S14 (see the Supporting Information).

Discussion

Bonding in the phenate anions

When analysing the structures of the various salts described, it quickly became apparent that in almost every case, the C—O bond of the phenate was shorter than might otherwise be expected, being found between 1.291(2) and 1.312(3) Å. The only exception was in the neutral pentafluorophenols in **2** and **3**, not discussed further, where the distances were 1.3391(17) and 1.335(2) Å, respectively. The C—O length in pentafluorophenol itself is around 1.37 Å (data exist for >1 polymorph).

The contraction is consistent with the development of C=O π-bond character and prompted examination of the C—C bond lengths in the ring (Table 1). Thus, in all cases but **1** and **4**, there was evidence for changes in the C—C bond lengths to those of a structure that could be described as either fully delocalised (Figure 20a: **2** (phenate ring), **3**, **6**, **7**, **8**, **13**) or partially delocalised (Figure 20b: **5**, **9**, **10**, **11**, **12**, **14**). 'Full delocalisation' means that the C1—C2 bond was statistically longer than both C2—C3 and C3—C4 bonds, whereas 'partial delocalisation' means that the C2—C3 bond was statistically shorter than those of C1—C2 and C3—C4. The distinction between the two classes takes the values of the estimated standard deviation (esd) into account, which in turn depend on the R factor. That said, it is felt that, in reality, probably all of the structures fall into the 'fully delocalised' category. Interrogation of the Cambridge Crystallographic Database shows rather few structures

Table 1. Key phenate bond lengths [Å] and bond angles [°] in the complexes studied. Atom numbers are those from Figure 20.

	1	2 (phenol)	2 (phenate)	3 (phenol)	3 (phenate)	4	5	6	7
C1=O	1.311(3)	1.3391(17)	1.3116(16)	1.335(2)	1.301(2)	1.306(2)	1.304(5)	1.297(5)	1.297(2)
C1—C2	1.400(3)/1.404(3)	1.390(2)/1.400(2)	1.406(2)/1.414(2)	1.392(2)/1.384(2)	1.402(2)/1.404(2)	1.405(3)/1.409(3)	1.412(5)/1.409(5)	1.404(4)	1.406(3)/1.408(3)
C2—C3	1.384(3)/1.373(3)	1.385(2)/1.3874(19)	1.3866(19)/1.3833(19)	1.376(2)/1.384(2)	1.377(2)/1.373(2)	1.376(3)/1.379(3)	1.380(6)/1.382(5)	1.371(5)	1.376(3)/1.370(3)
C3—C4	1.377(4)/1.376(3)	1.383(2)/1.378(2)	1.377(2)/1.384(2)	1.370(2)/1.374(2)	1.377(2)/1.372(2)	1.385(3)/1.390(3)	1.388(5)/1.395(6)	1.379(4)	1.387(3)/1.389(3)
Angle	H···O···H		H···O···H		H···O···H	H···O···H	H···O···H (polymer)	H···O···H	H···O···H
	96		119		96	107	104 116	110	106

	8[a]	9[a]	10	11	12	13	14	15	16
C1=O	1.298(2)	1.3079(18)	1.291(2)	1.292(3)	1.298(2)	1.301(2)	1.301(5)	1.242(3)	1.240(2)
C1—C2	1.405(3)/1.403(3)	1.406(2)/1.402(2)	1.406(2)/1.412(2)	1.409(3)/1.413(4)	1.417(3)/1.407(3)	1.404(3)/1.406(3)	1.413(6)/1.406(6)	–	–
C2—C3	1.376(3)/1.374(3)	1.376(2)/1.382(2)	1.378(2)/1.375(2)	1.370(4)/1.368(4)	1.367(3)/1.376(3)	1.374(3)/1.376(3)	1.367(6)/1.370(6)	–	–
C3—C4	1.382(3)/1.383(3)	1.385(2)/1.381(2)	1.395(2)/1.375(2)	1.386(3)/1.390(4)	1.385(3)/1.393(3)	1.382(3)/1.378(3)	1.400(6)/1.385(5)	–	–
Angle	H···O···H	H···O···H	H···O···I	H···O···I	H···O···H	H···O···H (polymer)	H···O···H	H···O···H	H···O···I
	94 104	93 103	100	100	105	136	103	76	83

[a] For **8** and **9** there are two H···O···H angles as there are two, independent dimers in the asymmetric unit. In each case, the smaller value refers to the hydrogen-bonded dimer where there is, in addition, a halogen bond to iodine. In addition, each structure has two H···O···I angles: **8**: 84° and 114° and **9**: 106° and 128°.
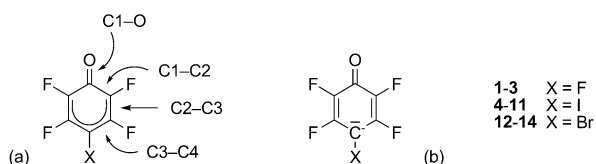
Figure 20. (a) The 'fully' delocalised and (b) the 'partially' delocalised bonding motifs found in the various phenate anions. Note that C1, C2, etc., are generic labels and that the actual atom numbers will vary from structure to structure.

of the free pentafluorophenate anion where such delocalisation is observed, although the papers tend to contain no comments. However, the Database also shows that such delocalisation is quite common in phenate anions.

To probe this further, the geometry of pentafluorophenol, its anion and the anion of both the 4-iodotetrafluorophenate and 4-bromotetrafluorophenate anions were optimised at the MP2-(Full) level of theory and their electronic structures were subjected to natural bond orbital (NBO) analyses. Cartesian coordinates of the optimised geometries can be found in Table S3 of the Supporting Information. Data were also obtained for 4-chlorotetrafluorophenol/4-chlorotetrafluorophenate and 4-iodotetrafluorophenol and 4-bromotetrafluorophenol and are included as Figure S15 for completeness (see the Supporting Information). Thus, computational results (Figure 21) show the shortening of the C–O bond on ionisation and are also consistent with a 'fully' delocalised structure.

The results of the NBO analyses were utilised to probe further the quinoidal type structure. In the case of the phenol, the π-occupancies of the ring C–C bonds were observed to be between 1.67 and 1.71, which is consistent with a fully delocalised structure with no π-occupancy of the C–O bond. However, in the phenate anion, the π-occupancy of the C–O bond became 1.99, whereas that for C2–C3 was found to be 1.79 and C1–C2 and C3–C4 were found not to have π-occupancy, consistent with the quinoidal arrangement. A table containing calculated NBO values for each phenol/phenate pair can be found in the Supporting Information as Table S2.

Examination of the electrostatic surface potentials (ESPs) of the phenols and phenates provides further insights into their
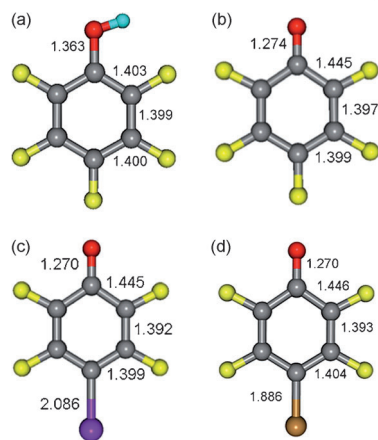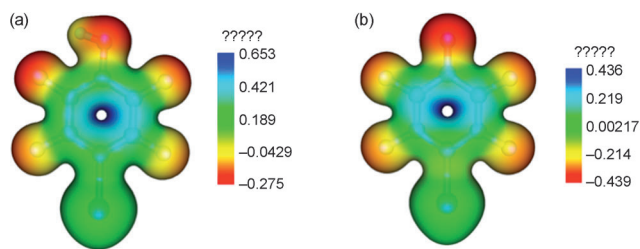

Figure 22. Electrostatic surface potentials for (a) 4-iodotetrafluorophenol and (b) the 4-iodotetrafluorophenate anion mapped on the respective 0.03 Hartree–Fock (HF) total electronic density isosurfaces.

electronic structures. Examples for 4-iodotetrafluorophenol/4-iodotetrafluorophenate are given in Figure 22 (other ESPs are included in Figure S16 in the Supporting Information). Deprotonation of the phenols to give the corresponding phenate leads to a more negative potential around the oxygen atom and, as the halogen in the para position becomes more polarisable, the potential around the halogen becomes more positive in the phenol. However, in the phenate, the positive electrostatic potential around the halogen decreases and, in the cases of F and Cl, becomes negative.

Bonding motifs in the structures

In the discussion that follows, the ketonic nature of the C–O bond is important as it allows comparison with the interactions between the amide carbonyl of a protein chain and bromo compounds as discussed by Ho and co-workers.[17,18]

The structures of all complexes with the exception of **10** and **11** reveal a strong preference for the phenate oxygen atom to accommodate two hydrogen-bond donors in the plane of the ring, so much so that in **2** and **3** a neutral pentafluorophenol co-crystallises to take up the second of these positions in the absence of a second ammonium hydrogen atom. This is consistent with the phenate anion having developed C=O bond character, which would lead to the presence of two sp^2 orbitals in the plane of the ring. This shows a parallel with the co-crystal structures in Figure 1, where there are two halogen bonds into lone-pair sp^2 orbitals on a carbonyl oxygen atom, and is consistent with experiments in the gas phase, which showed that FCl will form a halogen bond with the lone pairs of electrons of the carbonyl oxygen atom of formaldehyde with a C=O···Cl angle of 110.9°.[32] Interaction with the lone pairs of electrons was found to take precedence over interactions with the π electrons.

To probe this further, the HF molecular orbitals at the MP2-(Full) optimised geometries were localised by using the Edmiston–Ruedenberg localisation procedure. The results are illustrated for the iodotetrafluorophenate anion. Figure 23 a and b shows the presence of sp^2 orbitals on oxygen, clearly consistent with the strong preference shown in the crystal structures for two hydrogen-bond donors bound to oxygen in the plane of the ring.

The majority of cations used were secondary amines, meaning that there were two N–H hydrogen atoms at the cationic centre and so formation of the [2+2], hydrogen-bonded dimer

Figure 21. MP2(Full)-optimised geometries: C–C and C–O bond lengths (in Å) of (a) pentafluorophenol, (b) the pentafluorophenate anion, (c) the 4-iodotetrafluorophenate anion and (d) the 4-bromotetrafluorophenate anion.
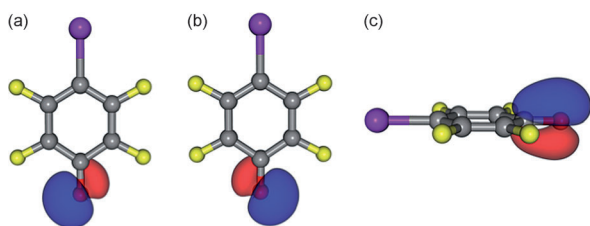
Figure 23. Representations of (a, b) the localised molecular orbitals (LMOs) corresponding to the lone electron pairs on O and (c) the π orbital on the C=O bond. The orbitals are represented as blue/red isosurfaces at orbital values of ± 0.05 (e/bohr^3)$^{-1/2}$.

Figure 24. Possible arrangements of hydrogen and halogen bonding at amide oxygen atoms showing (a) both in plane and (b) both out of plane with respect the amide link. After Ho and co-workers.[18]

is readily rationalised. However, use of a tertiary amine means that there is only one such hydrogen atom available and so in **10** and **11**, in-plane hydrogen and halogen bonds are formed (Figures 13 and 14), whereas in the case of **5**, there is a second N—H hydrogen atom available and so a linear polymer is seen (Figures 6 and S4a in the Supporting Information), which also provides for two hydrogen bonds at oxygen.

Then, considering **6** and **7**, the presence of a secondary ammonium cation allows for the formation of the [2+2] hydrogen-bonded dimer, but in the case of **7**, the thiomorpholinium cation also contains a sulfur atom that then forms a halogen bond to the phenate iodine atom, leading to a polymeric structure as shown in Figure 9.

However, in the case of **8** (pyrrolidium cation) and **9** (morpholinium cation), although the expected [2+2] dimer is indeed observed, examination of the structure shows that there is also an intermolecular I···O halogen bond. This forms between the iodine atom of a neighbouring iodotetrafluorophenate anion (itself part of a [2+2] dimer) and a phenate oxygen atom of the hydrogen-bonded dimer, with the iodine atom approaching out of the plane of the phenate ring (Figures 10b, 11 and 12). Interaction of the iodine atom with the oxygen atom uses the π-system of the C=O bond as illustrated in Figure 23c. So far as we are aware, such a combined hydrogen and halogen-bonding motif is without precedent in the literature of synthetic co-crystals.

Comparison with the motifs described by Ho and co-workers is then instructive. They first described systems mined from the Protein Data Bank (PDB) in which there was halogen bonding by Cl, Br or I to carbonyl oxygen atoms, almost all of which were associated with amide links in the peptide chain. In these cases and considering only the halogen···oxygen interaction, iodine showed a very strong preference for binding into the π-system of the C=O bond, whereas for bromine the preference in favour of binding to the π-system over binding to the lone pairs on oxygen was appreciably smaller, albeit over a smaller data set.[17] They then went on to mine data from the PDB for a series of protein–ligand combinations containing short X···O interactions.[18] This study showed that when only hydrogen bonding was present, the hydrogen bond formed preferentially directly opposite to the C=O bond and, as such, in the plane of the amide bond. However, in cases where there was both hydrogen and halogen bonding to the oxygen atom, then either the halogen would approach from the plane above the amide bond and the hydrogen bond would be found below
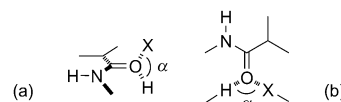
the same plane (Figure 24a), or both the halogen and hydrogen bond would be found bound to the oxygen in the plane of the amide bond (Figure 24b). In the majority of cases, the angle, α, was found to be between 75 and 90°, leading them to propose that the hydrogen and halogen bonds, when both present, should be regarded as orthogonal. Indeed, this idea was supported further by calculations, which showed that the energy of a hydrogen bond between two amide units was unaffected by the approach of the Br of bromobenzene to the hydrogen-bond acceptor (oxygen), and, similarly, the energy of interaction between the hydrogen-bond acceptor (oxygen) and a halogen-bonded bromine atom was unaffected by the length of the hydrogen bond to oxygen. For comparison, the strength of one hydrogen bond to oxygen was affected appreciably by the presence of a second hydrogen bond.

To make an even more direct comparison between the biological and synthetic systems, this study allowed the amides N-methylacetamide and N-methylbenzamide to co-crystallise with 1,4-diiodotetrafluorobenzene. The N-methylacetamide hydrolysed during crystallisation to give acetamide and the structure of the resulting co-crystal (**15**) showed sheets made up of hydrogen-bonded acetamides (Figure 18a) linked by the aromatic diiodide through I···O halogen bonding into the π-system of the amide carbonyl group (Figure 18b). N-Methylbenzamide did not hydrolyse during crystallisation and the structure also showed a one-dimensional, sheet-like arrangement but with one hydrogen atom fewer available for hydrogen bonding. Again, I···O halogen bonding into the π-system of the amide carbonyl held the sheets together.

These structures provide an excellent link between the biological systems and the co-crystal salts of the amine/phenol combinations as now described. Thus the N-methylbenzamide structure **16** mirrors the behaviour described by Voth et al. in having effectively orthogonal halogen and hydrogen bonding with an H···O···I angle of 83.0° (arrangement as in Figure 23b), which agrees well with the modal angle they report in such cases. Then there are the cases of **10** and **11**, where in each there is also a single hydrogen atom available for hydrogen bonding and so both a hydrogen and halogen bond are seen with the H···O···I angle = 100(1)° in each case. These can also be regarded as orthogonal, but in this case they exist in the plane of the phenate ring, an arrangement that would not be possible in **16** on steric grounds.

However, in **15**, although there is also an I···O halogen bond into the C=O π-system, there are, in addition, two hydrogen bonds that bind into the lone-pair sp^2 orbitals on the amide oxygen atom, a motif that is not found in the biological systems as the amide link contains a single hydrogen atom available for hydrogen bonding and the close approach of two hydrogen atoms is likely disfavoured sterically. As noted already,

this motif is also found in **8** and **9**. In these three structures, the H···O···H angle in the [2+2] dimer is 76° (**15**) and 93.5° (**8** and **9**), whereas in structures of 4-halotetrafluorophenates where there is a [2+2] dimer and no halogen bonding (**4**–**7** and **12**–**14**), then the same angle is in the range 100 to 107°.[33] Thus, in contrast to the calculations reported by Voth et al., in this case the hydrogen and halogen bonding are not orthogonal as it is evident that the H···O···H angle is appreciably smaller where there is additional I···O halogen bonding. This is shown elegantly in the structures of **8** and **9**, where in each case there are two, independent [2+2] dimers and, in the dimer where there is no halogen bond, the H···O···H angle is 103.5°, whereas in the other (which is halogen bonded) the angle is 93.5°.[34]

In the original paper by Auffinger et al.[17] and to an extent in the study by Voth et al.,[18] significant emphasis was placed on biological Br···O halogen bonds, whereas this synthetic study has concentrated on iodo materials. To this end, salts **12** to **14** were obtained and it is noteworthy that, save for the Type I Br···Br interactions in **13** (Figure 17 a), no other short contacts to Br are seen. In general terms, halogen bonds to bromine are expected to be weaker than iodine analogues and one very simple illustration of this is in the comparison between the 2:1 complexes formed between 4-alkoxystilbazoles and 1,4-diiodo- and 1,4-dibromo-tetrafluorobenzene. Thus, in both cases 2:1 co-crystals are obtained, but only the complex of the diiodotetrafluorobenzene showed liquid crystal properties as the analogous dibromotetrafluorobenzene complex fell apart on heating, suggesting weaker halogen bonding.[35]

While it is recognised that there are many factors that can affect the intermolecular interactions observed in a co-crystal system, it is interesting that analogous halogen-bonding motifs are not seen in any of **12** to **14**. What this may point to is the fact that in protein systems, interactions that form can be a result of a range of steric and allosteric factors related to secondary and tertiary structures, and indeed Voth et al. draw attention to α-helices and β-sheets in their discussions.[18] Therefore, although the structures reported here offer synthetic analogues that can help in the interpretation and understanding of the halogen bonds found in proteins, it is clear that the analogy cannot be taken too far given the structural complexity in proteins at the secondary and tertiary level.

Of course, one might then go further and argue that in the solid-state structures of molecular species, the importance or not of any given intermolecular, interatomic contact(s) may be a delicate function of the enthalpic contribution made to the lattice energy when compared with the general driving force for efficient molecular packing, which may lead to such interactions occurring by accident rather than design.

Conclusion

In this extensive and systematic study of salts and co-crystals formed mainly between 4-halotetrafluorophenols and cyclic amines, it is noted that in all cases the phenate ion formed adopts a delocalised, Meissenheimer-like structure in which double-bond character develops in the C—O bond. This is sup-

ported by calculations at the MP2 level of theory and then explains the observation that the hydrogen-bonding motifs of these phenates are dominated by interaction with the lone-pair sp^2 orbitals on the oxygen atoms. Where there are insufficient hydrogen atoms to allow formation of two hydrogen bonds per oxygen atom, then both hydrogen *and* halogen bonding into the sp^2 orbitals is observed.

However, in some cases where there are already two hydrogen bonds to an oxygen atom, an additional I···O halogen bond forms representing an interaction between the electrophilic iodine atom of the 4-iodotetrafluorophenate and the π-bonding orbital or the carbonyl group. The broader significance of this observation is that not only is the motif without precedent in studies of halogen-bonded materials, but it also presents a synthetic analogy with observations of halogen bonding in the structures of proteins as described by Ho and co-workers.[16–18] Moreover, while the synthetic studies can reproduce the orthogonality of hydrogen and halogen bonding proposed by Ho and supported by calculation, they also show that this orthogonality breaks down where there are simultaneously two hydrogen bonds and a halogen bond to oxygen.

Finally, structures obtained by using 4-bromotetrafluorophenol do not reproduce these motifs, an observation that may point to the greater importance of steric and allosteric factors in determining intermolecular arrangements in protein systems.

Experimental Section

4-Iodotetrafluorophenol was prepared as described in the literature.[36] All other reagents were obtained commercially and were used as obtained.

General remarks on co-crystallisation experiments

In a typical co-crystallisation experiment, vapour diffusion techniques were used. The components were dissolved in a small volume of common solvent, and placed inside a tablet tube inside a vial and the tablet tube was then covered with aluminium foil, which was punctured by using a needle. The anti-solvent (ca. 2 cm^3) was added to the vial, which was then sealed with a cap and covered in parafilm to prevent evaporation of the solvents. Solvents and anti-solvents are given in Table 2.

Table 2. Solvent systems used in the crystallisations.

	Solvent	Anti-solvent
1	dichloromethane	cyclohexane
2	THF	cyclohexane
3	THF	none
4	methanol	toluene
5	THF	hexane
6	THF	cyclohexane
7	methanol	iPr$_2$O
8	chloroform	cyclohexane
9	THF	cyclohexane
10	THF	diethyl ether
11	chloroform	cyclohexane
12	acetonitrile	none
13	acetonitrile	none
14	THF	none
15	dichloromethane	none
16	dichloromethane	none

Single-crystal X-ray structures were determined as described elsewhere;[37] CCDC deposition numbers are given in Table S1.

Computational procedure

The geometries of pentafluorophenol, its anion, and the 4-halotetrafluorophenols and their anions were optimised at the MP2(Full) level of theory (second-order Møller–Plesset perturbation theory, all electrons correlated), within the aug-cc-pVDZ basis (aug-cc-pVDZ-PP on I), by using Gaussian 09.[38] This basis set combination was used in all calculations reported in this paper. Vibrational frequencies were calculated to ensure that the optimised geometries correspond to local minima on the potential energy surface. The Hartree–Fock (HF) molecular orbitals were localised by using the Edmiston–Ruedenberg localisation procedure implemented in GAMESS-US.[39] The electrostatic surface potentials (ESPs) associated with the total HF electronic densities were calculated at the respective MP2(Full) optimised geometries, by using Molekel.[40] Molekel was also employed in order to visualise other computational results.

Acknowledgements

[1] K. Rissanen, *CrystEngComm* **2008**, *10*, 1107–1113.
[2] A. Priimagi, G. Cavallo, P. Metrangolo, G. Resnati, *Acc. Chem. Res.* **2013**, *46*, 2686–2695; P. Metrangolo, H. Neukirch, T. Pilati, G. Resnati, *Acc. Chem. Res.* **2005**, *38*, 386–395.
[3] A. C. Legon, *Phys. Chem. Chem. Phys.* **2010**, *12*, 7736–7747.
[4] T. M. Beale, M. G. Chudzinski, M. G. Sarwar, M. S. Taylor, *Chem. Soc. Rev.* **2013**, *42*, 1667–1680.
[5] P. Politzer, J. S. Murray, T. Clark, *Phys. Chem. Chem. Phys.* **2013**, *15*, 11178–11189.
[6] H. L. Nguyen, P. N. Horton, M. B. Hursthouse, A. C. Legon, D. W. Bruce, *J. Am. Chem. Soc.* **2004**, *126*, 16–17.
[7] B. K. Saha, A. Nangia, J. Nicoud, *Cryst. Growth Des.* **2006**, *6*, 1278–1281.
[8] E. Cariati, G. Cavallo, A. Forni, G. Leem, P. Metrangolo, F. Meyer, T. Pilati, G. Resnati, S. Righetto, G. Terraneo, E. Tordin, *Cryst. Growth Des.* **2011**, *11*, 5642–5648.
[9] L. Meazza, J. A. Foster, K. Fucke, P. Metrangolo, G. Resnati, J. W. Steed, *Nat. Chem.* **2012**, *5*, 42–47.
[10] A. Caballero, F. Zapata, N. G. White, P. J. Costa, V. Felix, P. D. Beer, *Angew. Chem.* **2012**, *124*, 1912–1916; *Angew. Chem. Int. Ed.* **2012**, *51*, 1876–1880.
[11] M. Fourmigué, *Struct. Bonding (Berlin)* **2008**, *126*, 181–207.
[12] P. Metrangolo, Y. Carcenac, M. Lahtinen, T. Pilati, K. Rissanen, A. Vij, G. Resnati, *Science* **2009**, *323*, 1461–1464.
[13] A. Abate, M. Brischetto, G. Cavallo, M. Lahtinen, P. Metrangolo, T. Pilati, S. Radice, G. Resnati, K. Rissanen, G. Terraneo, *Chem. Commun.* **2010**, *46*, 2724–2726.
[14] J. Martí-Rujas, L. Meazza, G. K. Lim, G. Terraneo, T. Pilati, K. D. M. Harris, P. Metrangolo, G. Resnati, *Angew. Chem.* **2013**, *125*, 13686–13690; *Angew. Chem. Int. Ed.* **2013**, *52*, 13444–13448.
[15] F. Kniep, S. H. Jungbauer, Q. Zhang, S. M. Walter, S. Schindler, I. Schnapperelle, E. Herdtweck, S. M. Huber, *Angew. Chem.* **2013**, *125*, 7166–7170; *Angew. Chem. Int. Ed.* **2013**, *52*, 7028–7032.
[16] M. R. Scholfield, C. M. V. Zanden, M. Carter, P. S. Ho, *Protein Sci.* **2013**, *22*, 139–152.
[17] P. Auffinger, F. A. Hays, E. Westhof, P. S. Ho, *Proc. Natl. Acad. Sci. USA* **2004**, *101*, 16789–16794.
[18] A. R. Voth, P. Khuu, K. Oishi, P. S. Ho, *Nat. Chem.* **2009**, *1*, 74–79.
[19] See, for example: R. Wilcken, M. O. Zimmermann, A. Lange, A. C. Joerger, F. M. Boeckler, *J. Med. Chem.* **2013**, *56*, 1363–1388; L. A. Hardegger, B. Kuhn, B. Spinnler, L. Anselm, R. Ecabert, M. Stihle, B. Gsell, R. Thoma, J. Diez, J. Benz, J.-M. Plancher, G. Hartmann, D. W. Banner, W. Haap, F. Diederich, *Angew. Chem.* **2011**, *123*, 329–334; *Angew. Chem. Int. Ed.* **2011**, *50*, 314–318; A. R. Voth, F. A. Hays, P. S. Ho, *Proc. Natl. Acad. Sci. USA* **2007**, *104*, 6188–6193; M. Carter, A. R. Voth, M. R. Scholfield, B. Rummel, L. C. Sowers, P. S. Ho, *Biochemistry* **2013**, *52*, 4891–4903.
[20] O. Hassel, K. O. Strømme, *Acta. Chem. Scand.* **1959**, *13*, 275–280.
[21] R. Lo, A. Ballabh, A. Singh, P. Dastidar, B. Ganguly, *CrystEngComm* **2012**, *14*, 1833–1841.
[22] J.-L. Syssa-Magalé, K. Boubekeur, B. Schöllhorn, *J. Mol. Struct.* **2005**, *737*, 103–107.
[23] J. N. Moorthy, P. Venkatakrishnan, P. Mal, S. Dixit, P. Venugopalan, *Cryst. Growth Des.* **2003**, *3*, 581–585.
[24] O. Bolton, K. Lee, H.-J. Kim, K. Y. Lin, J. Kim, *Nat. Chem.* **2011**, *3*, 207.
[25] S. K. Maity, S. Bera, A. Paikar, A. Pramanik, D. Haldar, *Chem. Commun.* **2013**, *49*, 9051–9053.
[26] H. S. El-Sheshtawy, B. S. Bassil, K. I. Assaf, U. Kortz, W. M. Nau, *J. Am. Chem. Soc.* **2012**, *134*, 19935–19941.
[27] C. Präsang, H. L. Nguyen, P. N. Horton, A. C. Whitwood, D. W. Bruce, *Chem. Commun.* **2008**, 6164–6166.
[28] M. Gdaniec, *CrystEngComm* **2007**, *9*, 286–288.
[29] C. B. Aakeröy, S. Panikkattu, P. D. Chopade, J. Desper, *CrystEngComm* **2013**, *15*, 3125–3136.
[30] D. Zobel, P. Luger, W. Dreissig, T. Koritsanszky, *Acta Crystallogr. Sect. B* **1992**, *48*, 837–848 (R_3c polymorph); J. W. Bats, M. C. Haberecht, M. Wagner, *Acta Crystallogr. Sect. E* **2003**, *59*, o1483–o1485 (*Pccn* polymorph).
[31] L. Leiserowitz, M. Tuval, *Acta Crystallogr. Sect. B* **1978**, *34*, 1230–1247.
[32] A. C. Legon, *Struct. Bonding (Berlin)* **2008**, *126*, 17–24.
[33] The exception is the angle of 136° in **13** where the hydrogen bonding describes a polymeric arrangement.
[34] The two angles are recorded by Mercury as 94(1)° for **8** and 93(1)° for **9** so given the esds, a simple average is quoted. Mercury is available free-of-charge from http://www.ccdc.cam.ac.uk.
[35] D. W. Bruce, P. Metrangolo, F. Meyer, C. Präsang, G. Resnati, A. C. Whitwood, *New J. Chem.* **2008**, *32*, 477–482.
[36] J. Wen, J. Yu, Q. Chen, *J. Mater. Chem.* **1994**, *4*, 1715–1717.
[37] J. P.-W. Wong, A. C. Whitwood, D. W. Bruce, *Chem. Eur. J.* **2012**, *18*, 16073–16089.
[38] Gaussian09, Revision A.1, M. J. Frisch, G. W. Trucks, H. B. Schlegel, G. E. Scuseria, M. A. Robb, J. R. Cheeseman, G. Scalmani, V. Barone, B. Mennucci, G. A. Petersson, H. Nakatsuji, M. Caricato, X. Li, H. P. Hratchian, A. F. Izmaylov, J. Bloino, G. Zheng, J. L. Sonnenberg, M. Hada, M. Ehara, K. Toyota, R. Fukuda, J. Hasegawa, M. Ishida, T. Nakajima, Y. Honda, O. Kitao, H. Nakai, T. Vreven, J. A. M., Jr., J. E. Peralta, F. Ogliaro, M. Bearpark, J. J. Heyd, E. Brothers, K. N. Kudin, V. N. Staroverov, R. Kobayashi, J. Normand, K. Raghavachari, A. Rendell, J. C. Burant, S. S. Iyengar, J. Tomasi, M. Cossi, N. Rega, J. M. Millam, M. Klene, J. E. Knox, J. B. Cross, V. Bakken, C. Adamo, J. Jaramillo, R. Gomperts, R. E. Stratmann, O. Yazyev, A. J. Austin, R. Cammi, C. Pomelli, J. W. Ochterski, R. L. Martin, K. Morokuma, V. G. Zakrzewski, G. A. Voth, P. Salvador, J. J. Dannenberg, S. Dapprich, A. D. Daniels, Ö. Farkas, J. B. Foresman, J. V. Ortiz, J. Cioslowski, D. J. Fox, Gaussian, Inc., Wallingford CT, **2009**.
[39] GAMESS, 21 Nov, M. W. Schmidt, K. K. Baldridge, J. A. Boatz, S. T. Elbert, M. S. Gordon, J. J. Jensen, S. Koseki, N. Matsunaga, K. A. Nguyen, S. Su, T. L. Windus, M. Dupuis, J. A. Montgomery, **1995**.
[40] Molekel 5.4.0.8, U. Varetto, Swiss National Supercomputing Centre, Manno (Switzerland), **2009**.